ADVANCED FUNCTIONAL MATERIALS
www.afm-journal.de

Well-Ordered and High Density Coordination-Type Bonding to Strengthen Contact of Silver Nanowires on Highly Stretchable Polydimethylsiloxane

Hanleem Lee, Keunsik Lee, Jin Taek Park, Woon Chun Kim, and Hyoyoung Lee**

Recently, Ag nanowires (AgNWs) has had a great interest as a conducting material for flexible and transparent devices, but it still shows several problems such as the ultimate detachment of AgNWs from substrate and a high contact resistance on AgNW junctions. Therefore, the novel concept to enhance permanent and closed attachment of AgNWs by silane modification to polydimethylsilaoxane (PDMS) substrate well known as high stretchable film with extremly low adhesive is suggested. According to this experiment, higher sigma (σ)-donating ability and hydrophilicity indicate better electrical and mechanical properties in real device. Especially, densely amine self-assembled PDMS surface exhibits the strongest contact force to the AgNWs, especially for junction side, and the longest maintenance of hydrophilicity by coordination-type bonding. In addition, AgNWs adhere permanently to stretchable substrates while simultaneously maintaining high transparency (87%) and high conductivity (27 Ω sq^{-1}). Consequently, the resulting AgNW film shows excellent mechanical durability which includes enhanced performance of both flexibility and stretchability.

1. Introduction

Need of studying new stretchable, transparent conductive films (TCFs) is being focused these days for stretchable electronic devices due to its numerous potential uses on many devices such as flexible displays, smart clothing, actuators, and energy storage devices. Nowadays, several stretchable conductive film applications have been introduced, such as a crumpled graphene actuators,[1] PEDOT:PSS-deposited FETs,[2] silver nanowire (AgNW) conductors, and wrinkled Al_2O_3-graphene-CNT transistors.[3] However, most applications were designed for non-transparency use, since the use of a large amount of conductive materials is required to fulfill a low sheet resistance (R_{sh}) during bending and stretching stress tests. Recently, polydimethylsiloxane (PDMS) has been widely investigated as a possible stretchable substrate for electronic devices.[4] PDMS is highly stretchable with linear extensions of up to 30%,[5] and has durability due to chemical inertness and thermal stability.[6] In addition, PDMS shows good transparency[7] and provides an easy and inexpensive fabrication process.[8] In spite of their numerous advantages, however, there have been few studies related to stretchable TCFs using PDMS due to poor control of its surface properties.[9] The conducting materials have extremely low adhesiveness on PDMS, because of their super hydrophobicity and fast hydrophobic recovery after surface hydrophilization. Additionally, they have a strong tendency to adsorb other molecules onto the surface, which can reduce the conductivity and stability of a stretchable device. Even worse, the conductive layers can easily be detached from the PDMS substrate with even weak mechanical forces applied to the conductive PDMS film, such as stretching force, providing no stretchable conductive films. To enhance the attachment of various kinds of materials on the PDMS surface, researchers has chosen the way to incubate material into PDMS or to modify PDMS surface. If conductive material is incubated in PDMS, however, it is hard to apply for the solar cell, field effect transistor (FET), and display that shows a laminated structure. Therefore, it must be satisfied to maintain electrical and mechanical stability within an opened system.[10] Until now, there was no such report about the good attachment of AgNWs to PDMS substrate not an incubating

H. Lee, Prof. H. Lee
Center for Smart Molecular Memory
Department of Energy Science
Sungkyunkwan University
2066, Seoburo, Jangan-gu, Suwon
Gyeonggi-do 440–746, Republic of Korea
E-mail: hyoyoung@skku.edu
Dr. W. C. Kim
Corporate R&D Institute
Samsung Electro-Mechanics
Suwon-si 443–743, Republic of Korea
E-mail: woonchun.kim@samsung.com
K. S. Lee, J. T. Park, Prof. H. Lee
Center for Smart Molecular Memory
Department of Chemistry
Sungkyunkwan University
2066, Seoburo, Jangan-gu, Suwon Gyeonggi-do 440–746
Republic of Korea
Prof. H. Lee
Center for Smart Molecular Memory
SKKU Advanced Institute of Nano Technology (SAINT)
Sungkyunkwan University
2066, Seoburo, Jangan-gu, Suwon Gyeonggi-do 440–746
Republic of Korea

DOI: 10.1002/adfm.201303276

system, nor have there been studies on the changes in the electrical properties, depending on the interfacial states of conductive material and molecularly modified PDMS substrate. It is highly necessary to investigate how to attach AgNWs on PDMS permanently, even when the TCF is stretched and contracted.

Herein, we introduce a novel, stretchable AgNW PDMS TCF, using several different kinds of molecularly self-assembled polar PDMS substrates. We carefully designed a molecularly silanized PDMS surface with different degree of sigma (σ)-donating polar ability that can give a permanent coordination-type bond[11] and high polarity on stretchable PDMS surfaces. The σ-donating polar head groups of the pre-silanized PDMS surface can tightly hold AgNWs through a dipole-dipole attraction, hydrogen bonding, and metal-ligand interaction, and can also squeeze AgNW junctions, providing a highly performed stretchable AgNW TCF. To investigate the adhesion of AgNWs on the strong σ-donating or weak σ-donating polar molecules on the molecularly self-assembled PDMS surface, various silane compounds having a strong σ-donor molecules including ([3-(2-aminoethylamino)propyl]trimethoxy silane ($Si(NNH_2)$), 3-aminopropyltriethoxysilane ($Si(NH_2)$), 3-mercaptopropyltrimethoxysilane (Si(SH)) and weak σ-donor molecules such as 3-glycidyloxypropyltrimethoxysilane (Si(O)) and 3-chloropropyltriethoxysilane (Si(Cl)) are chosen. It is highly expected that $Si(NNH_2)$ can have the strongest adhesion with high transparency, bendability, and strechability (Figure S2, Supporting Information).

2. Surface Modification

A schematic design of the main process to fabricate GO/AgNW/$Si(NNH_2)$/PDMS film is shown in **Figure 1**a. The surface of PDMS is firstly treated with plasma to make an exposed hydroxyl group, followed by immersion in $Si(NNH_2)$ solution.[12] AgNWs and GO were sequentially deposited on the silane-modified PDMS surface (see the Experimental Section for details). The resulting TCF shows a high transparency and high stretchability, as demonstrated in Figure 1a. A red LED lamp is connected to each side of the film, which was luminous during the bending and stretching tests (Videos S1 and S12, Supporting Information). The transmittance and reflectance are also measured with a UV-Vis spectrometer (Figure 1b). The sheet resistance (R_{sh}) of this film is 27 Ω sq^{-1} with 87% back transmittance at 550 nm, which represents a huge improvement in both sheet resistance and transparency while being compared

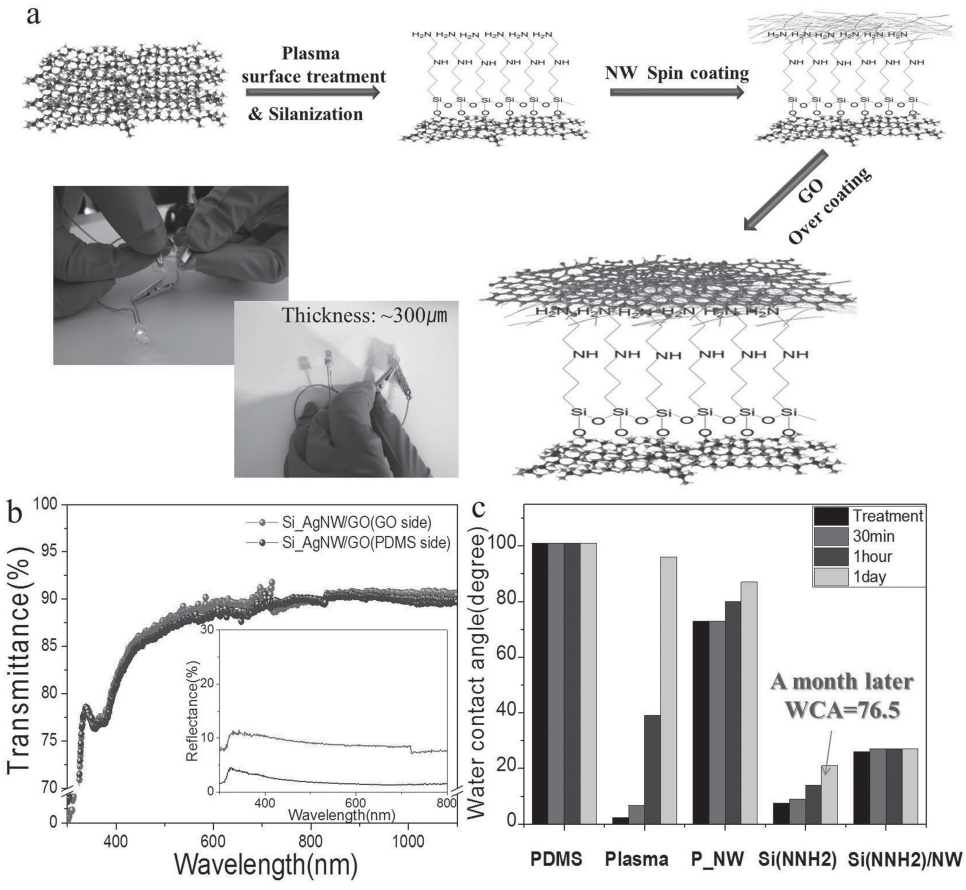

Figure 1. a) The fabrication procedure of stretchable TCF. The photos show an ON status of the LED light while the film is biaxially stretched to 30% (upper) and folded (bottom). b) Optical transmittance and reflection spectra of front side (red line) and back side (blue line) of GO/AgNW/$Si(NNH_2)$/PDMS. The inset indicates that the reflection spectrum of GO side is higher than that of the PDMS side. c) Water contact angles for several modified substrates: naive PDMS, plasma treated PDMS, NW deposited PDMS after Plasma (P_NW), silanized PDMS using [3-(2-aminoethylamino)propyl] trimethoxysilane ($Si(NNH_2)$), AgNW PDMS after plasma and silanized (Si(NNH2)/NW).

with conventional AgNW-based electrodes on PDMS (35 Ω sq^{-1} with ≈80% transmittance).[13] The durability of the hydrophilicity is presented in Figure 1c. Only the plasma-treated samples including P and P_NW PDMS have fast recovery of the hydrophobic features in comparison with the molecularly self-assembled silanized samples, such as Si(NNH_2) and Si(NNH_2)/NW. The water contact angle (WCA) of Si(NNH_2) PDMS increases very slowly, and takes a month to reach 76.7° under atmosphere, while the plasma-treated P sample takes less than a day. Surprisingly, the WCA of Si(NNH_2)/NW is maintained low at 26–27°, and is almost unchanged, while that of the P_NW PDMS is high at over 70°, and also increased from 73 to 87°, which indicates the very characteristic role of the NNH_2 functional head group in the AgNW. From these WCAs, we can partially summarize that coordination-type bonding between AgNWs and the strong σ-donating NNH_2 functional head group prevents self-healing into a hydrophobic PDMS surface by disturbing the migration of low-molar PDMS chains and leads to maintain a low WCA over long period.

3. Various Self-Assembly Silanized PDMS Series

To clearly understand the role of the silane compounds with different functional head groups in the AgNWs, various silanized PDMSs were prepared. Silane molecules with NNH_2, NH_2, Cl, SH, and O functional head groups were used to control interaction between AgNWs and the functional head groups, which help to keep good hydrophilicity. Optical images of various silanized PDMS films are shown in **Figure 2**a. The NNH_2-modified surface shows a large number of nanowires with their uniform alignment, while the NH_2-, SH-, and Cl-modified PDMS surfaces exhibit fewer nanowires with random positions. The AgNW networks of the O-modified surface and non-silanized surface are easily disconnected and/or aggregated, resulting in high R_{sh}. It is believed that this result comes from a lack of adhesion force of these functional head groups to the AgNWs, which is confirmed with AFM images showing obvious differences. The strong σ-donating hydrophilic surface of NNH_2 manifests as a uniform and interconnected network. AgNWs are strongly adhered to the molecularly NNH_2-silanized PDMS surface, so that the AFM images of the nanowire junctions show buckled structure, while the other images exhibit plenary stacked structure (Figure 2b). In addition, it seems that the surface-nanowire interval on the AgNW NNH_2-silanized PDMS film is fixed at approximately 11 nm by its strong adhesion force (**Figure 3**a). Surprisingly, the NH_2 and SH groups, which are well known as strong σ-donating functional groups, also exhibit plenary structure, which means that the adhesion force of NH_2 and SH groups to the AgNWs is weaker than that of the NNH_2 group. It is assumed that the density of NH_2 and SH head groups of silanized PDMS film is too low to hold AgNWs tightly, so that the coordination-type bonding strength is not enough to overcome the self-healing hydrophobicity of the PDMS surface. The XPS spectra of amine functional head groups on AgNWs support this fact. Regarding the concentration% of Ag and N atoms, the NNH_2 film shows much higher values than the NH_2 films (Figure S7, Supporting Information). Moreover, NNH_2 silane molecules seem to be well ordered on substrate since NNH_2 film has the lowest root mean square (RMS) surface roughness (Figure S5, Supporting Information). On the other hand, the Cl, O, and non-silanized PDMS films produce very blurry images due to the huge height differences and broad deviations of the surface-nanowire interval. Even after coating with GO, the AgNW junction of NNH_2 is more tightly stacked, leading to a decrease of the cross sectional height from 23.7 nm, without GO, to 17.8 nm with GO (Figure S6, Supporting Information). The resulting GO/AgNW/Si(NNH_2)/PDMS TCF produces the lowest R_{sh} of 27 Ω sq^{-1} (Figure 3b). Other films present high R_{sh}, however, even after GO coating, with values such as 184 Ω sq^{-1} (NH_2), 303 Ω sq^{-1}

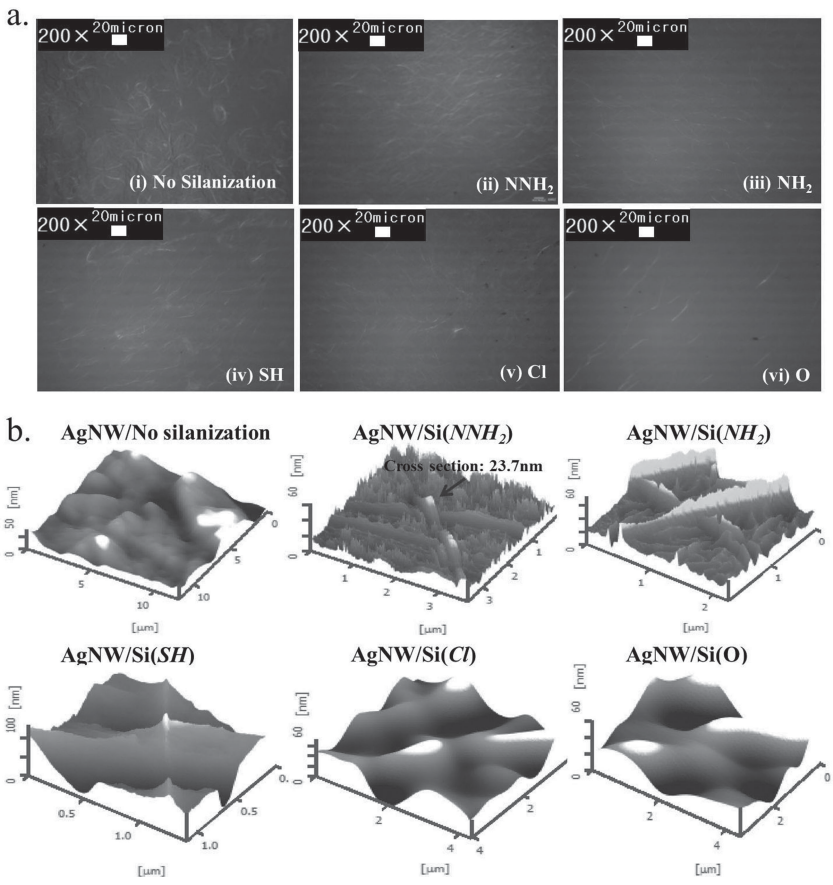

Figure 2. Characterization of various silanized PDMS surfaces. a) Optical micrographs of AgNW/no silanization (i), AgNW/Si(NNH_2) (ii), AgNW/Si(NH_2) (iii), AgNW/Si(SH) (iv), AgNW/Si(Cl) (v), AgNW/Si(O) (vi) on PDMS. b) AFM images of AgNW/Si(NNH_2), AgNW/Si(NH_2), AgNW/Si(SH), AgNW/Si(Cl), and AgNW/Si(O). AgNWs of NNH_2, NH_2, and SH silanized PDMS are imaged, while those of Cl, O, and non-silanized PDMSs were not readily apparent.

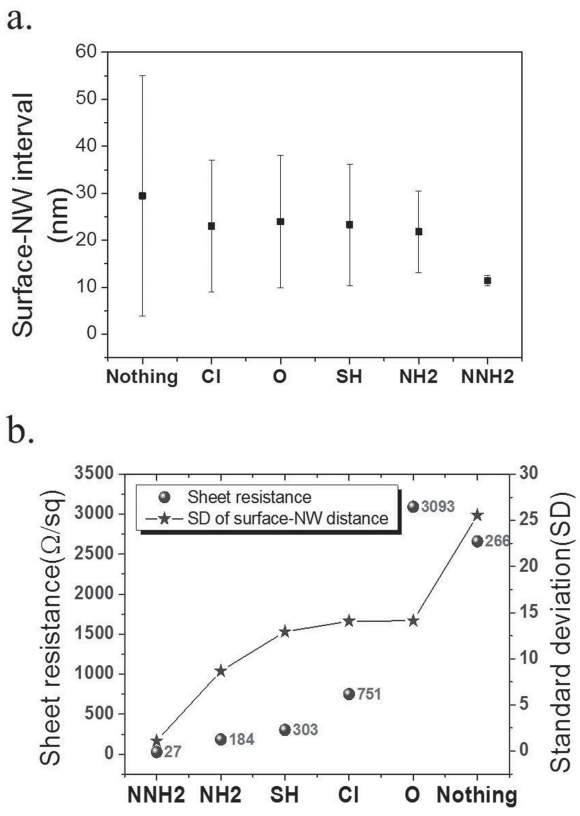

Figure 3. a) Plots of surface-nanowire intervals measured at 16 different places for various films: AgNW/no silanization (i), AgNW/Si(NNH_2) (ii), AgNW/Si(NH_2) (iii), AgNW/Si(SH) (iv), AgNW/Si(Cl) (v), AgNW/Si(O) (vi) on PDMS. Standard deviation (SD) of non-silane-treated PDMS is high (SD = 25.56) because the edge of nanowires float on air, while SD of NNH_2 film is low (SD = 1.01). b) Plots of standard deviation of surface-nanowire interval via different silane group and their corresponding sheet resistance values.

(SH), 751 Ω sq^{-1} (Cl), 3093 Ω sq^{-1} (O), and 2661 Ω sq^{-1} (non-silanized PDMS).

The XPS spectra of AgNWs placed on various silanized PDMS also show how the molecularly silanized PDMS can interact with AgNWs (**Figure 4**a,b). The XPS spectra reveal that the Ag 3d5/2 peak of the AgNW NNH_2 PDMS film is downshifted from 367.51 eV to 367.174 eV, which is a result of the doping effect of the NNH_2 functional head groups of the silane molecule. Amazingly, the downshift phenomena follows the tendency of a coordination-type bonding ability, which means that the order of the bond strength between the σ-donor functional head groups and the AgNWs is SH>NH_2>OEt>Cl.[14] It is strongly believed that the functional head groups of silane molecules alter the charge density of the silver nanowires. It is suggested that the interaction of the σ donor head group with silver metal is stronger, and the Ag-ligand binding energy should be reduced, representing the antibonding Ag-ligand characteristics on the LUMO of the neutral complex.[15] Notably, an Ag 3d5/2 peak of NNH_2 appears at 367.174 eV, which is lower than those of NH_2 and even SH. The contact force between the AgNWs and silanized PDMS surface is mainly affected by the density of the coordination-type bond, not the dipole-dipole interaction. Therefore, it is suggested that an evenly exposed surface with low RMS and an extra σ-bonding donor group (-N-) enhances the density of the coordination-type bonding on the interfacial states. This subsequently leads to a strong contact force, and makes the Ag d orbital of the NNH_2 film downshifted. In addition, when we observed metal Ag (368.2 eV for Ag 3d5/2, 374.2 eV for Ag 3d3/2) and Ag-X (367.5 eV for Ag 3d5/2, 373.5 eV for Ag 3d3/2) binding energy,[16] the NNH_2 film presents the largest ratio of [metal Ag]/[Ag-X] intensity, as predicted. It can be partially concluded that the NNH_2 PDMS film has the best interfacial adhesion among the 5 AgNW-silanized PDMS films. Raman-AFM measurement of the GO/AgNW/Silane/PDMS film was also carried out. The Raman map and its surface morphology are monitored to investigate exact G band shift, which can be used to compare the electrostatic interaction force between NNH_2 and NH_2, and also to estimate their contribution to the electric properties. The G band originated from the GO, which is directly exposed on the silanized PDMS film, is almost the same no matter how the NNH_2 or NH_2 films are used (Figure S8, Supporting Information). Nevertheless, the G band of the NNH_2 is more shifted from 1568 cm^{-1} to 1596 cm^{-1} than that of NH_2 from 1568 cm^{-1} to 1593 cm^{-1} in the case of the junction side (Figure 4d). The reason is that NNH_2 provides a better adhesive nanowire junction than NH_2, and the resulting strengthened adhesion provides a greater contribution for the doping effect of AgNW on GO.

4. Mechanical Stability

The bending and stretching properties were investigated using a custom-built set of bending machines, and the resulting electrical R_{sh} of the film is shown in **Figure 5**a. GO coated onto a molecularly silanized AgNW TCF is used, since AgNWs can be oxidized without any over-coating layer. Only 1 or 2 layers (≈1 nm) GOs are deposited for protection from oxidation, but not for enhancing the mechanical stability of the PDMS TCF.[17] The R_{sh} value of the AgNW/Si(NNH_2)/PDMS film with a GO over-coating layer is increased from 28 to 79 Ω sq^{-1} after 40% stretching, while that of AgNW/Si(NNH_2)/PDMS film without GO is increased from 31 to 92 Ω sq^{-1}, which means that both ratios increased by about 3 times, and their sheet resistances with and without GO were not changed much. Furthermore, the GO/AgNW/Si(NNH_2)/PDMS film is very stable regardless of the number of cycles. R_{sh} changes by only ≈0.2 over 1000 bending cycles, and the resistance is recovered after bending, indicating excellent durability. However, the SH, Cl, and non-modified PDMS films show dramatic changes, because of the low density of coordination bonding and high hydrophobicity. The stretchability with respect to uniaxial tensile strain ranging from 0 to 50% is also measured. The R_{sh} value during stretching is slowly increased within 40% and even the R_{sh} values upon releasing is similar with initial R_{sh} value ($\Delta R/R < 2$). When the PDMS film was fully released up to 50% tensile strain, the R_{sh} value sharply increases over 538 Ω sq^{-1} during stretching, but the R_{sh} value of the silanized PDMS after releasing from 50% tensile strain stretching decreases to 109 Ω sq^{-1}, which indicates an excellent stretchable AgNW silanized PDMS TCF (Figure S10, Supporting Information). Furthermore, our optimized film maintains around 50 Ω sq^{-1} sheet resistance even

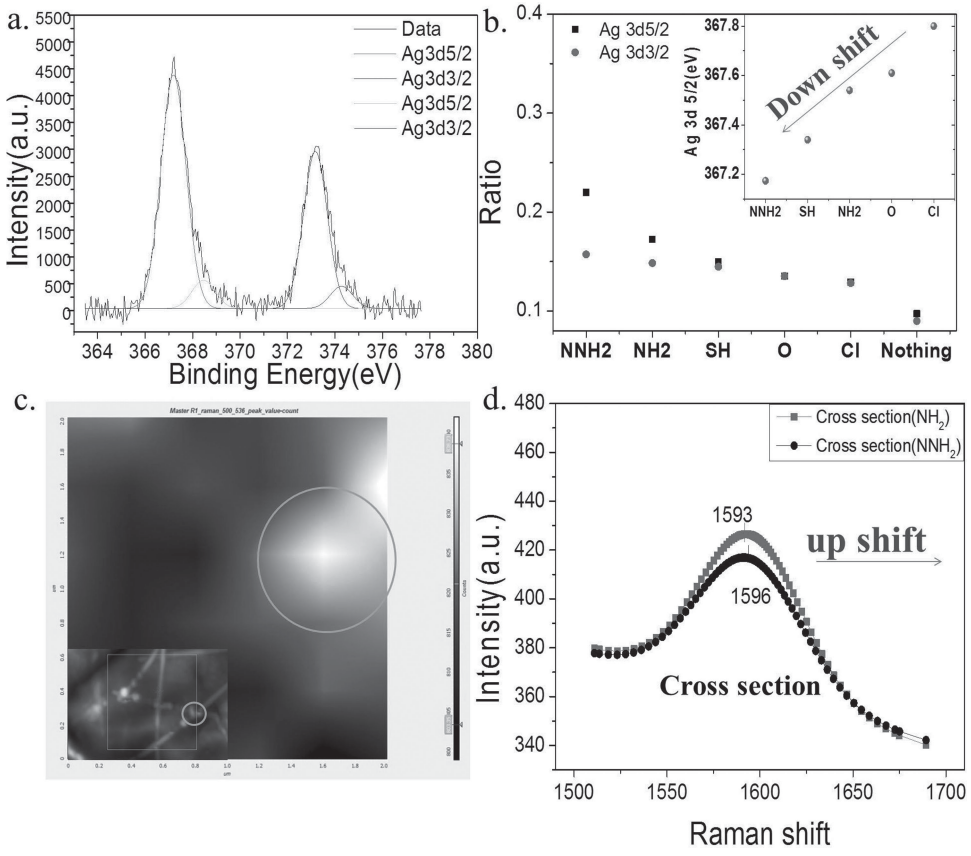

Figure 4. a) XPS spectra of AgNWs on NNH_2-modified surface at Ag3d region. b) Ratio of [metal Ag]/[Ag-ligand(X)] intensity of each film. The inset shows the peak shift of metal $Ag3d_{5/2}$ based on molecularly silanized PDMS. c) Raman map and AFM image of GO/AgNW/Si(NNH_2) film (2 μm × 2 μm). Raman spectra near 500–530, which is related to the Ag source, are extracted, and then their intensity changes appear as a color gradient. d) Raman spectra near G line to observe the degree of C-C bond stretching. NW junction on NNH_2 film has a 1596 cm^{-1} G peak, which is up-shifted relative to that of NH_2 film.

after 1,000 times of 30% stretching. At first stage, resistivity is dramatically changed because of residual strain on PDMS, while it is stabilized over 100 cycles (Figure 5b). Generally speaking, the resistance change under mechanical stresses can be easily explained by the disconnection of AgNW networks according to the delamination of the AgNW junctions as a result of weak adhesion to substrates.[18] The sheet resistance of a normal PDMS surface that does not have any coordination-type bonding to AgNWs cannot be returned to the original state, because AgNWs easily lift their head of AgNWs up from the substrate. However, AgNWs on NNH_2 film are not delaminated, even without GO, so that the network is easily restored by itself after removing mechanical forces, even though GO and/or AgNWs seem to be crumpled during bending or stretching.[19] To make sure, we observed the surface of the film using SEM images, before, during, and after stretchability tests (Figure 5c and Supporting Information Figure S9). The NH_2 film (Figure 5c,iv), which has low interaction between the substrate and over-coating layer, exhibits that AgNWs and GO are easily delaminated after stretching, leading to a rapid increase of the sheet resistivity. NNH_2 films (Figure 5c,ii,iii) also present several crumpled regions during mechanical stress, but we cannot observe any wavy GO or cracked AgNWs after the releasing step. Only several kink points were found compared with the initial state (Figure 5c,i), which may have been formed by residual strain, indicating that the conductivity was still good (51 Ω sq^{-1} with 30% stretching).

5. Touch Performance

Figure 6a shows a schematic of a stretchable capacitive AgNW-based touch pad. This pad consists of two different electrodes. The bottom electrode is our custom-made stretchable AgNW PDMS TCF, and the other is an Al membrane. An insulating GO film is applied as a separator, and its thickness is 100 um. Silver pastes are attached only at the edges of both electrodes of the film for applying an external current (Figure 6a,i,ii). A current is applied, and an output voltage is recorded from the device. The touch pad device is active through capacitive coupling[20] with a finger, as shown in the circuit design in Figure 6a iii. The finger contributes electrical impedance that is regarded as a body capacitor, and the capacitance can be increased.[21] To check whether our TCF can detect signals with or without a finger, we measured the voltage change, which is directly related to the capacitance. The NNH_2 film gives a high

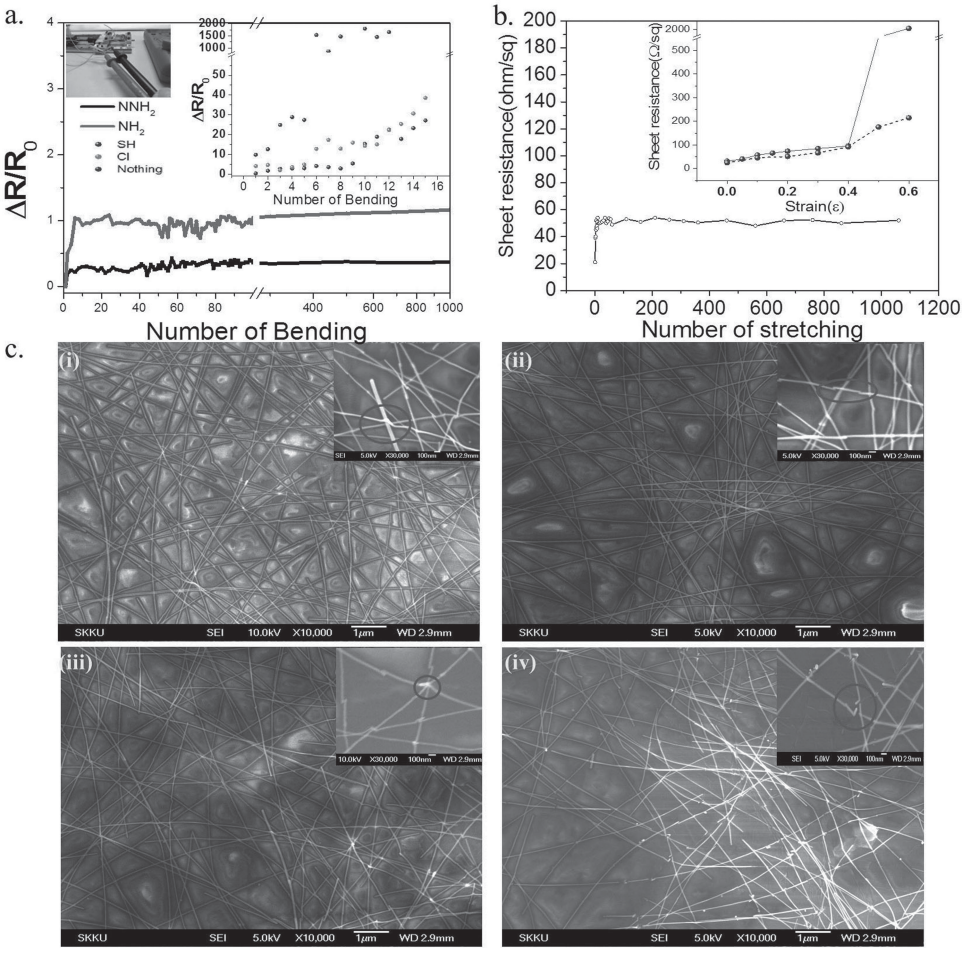

Figure 5. Electrical property. a) The ratios of sheet resistance change of GO/AgNW/SAM/PDMS films versus number of bending cycles. The ratios of sheet resistance for NNH_2 (black line) and NH_2 film (red line) show a little change, while that of SH, Cl, No silanized film present dramatic change. The inset provides a photo for a setup of the bending test. b) Stretchable stability along number of stretching ($\varepsilon = 30\%$), the inset illustrate the sheet resistance with respect to uniaxial strain during stretching (blue line) and after releasing (green line) for AgNW/Si(NNH_2)/PDMS film. c) SEM images of GO/AgNW/ Si(NNH_2)/PDMS film before (i), during (ii), after (iii) 20 times stretching ($\varepsilon = 30\%$), and that of GO/AgNW/ Si(NH_2)/PDMS film after 20 times stretching ($\varepsilon = 30\%$),(iv), respectively.

ON/OFF ratio (Figure 6b). In the "OFF" state (before a touch), the peak-peak voltage amplitude is 0.1 V, but in the "ON" state (after a touch), it increases significantly to 4.4 V. The ON/OFF voltage ratio of the NNH2 film is approximately 44 (Figure 6b). In addition, the touch pad gives a fast touch rate and high sensitivity. The electrical response with 0.5-Hz touch frequency is neat and repetitive[22] (Figure 6e). The results of the stretchable AgNW NNH_2 PDMS film are quite good, compared with those of the custom-made ITO/Glass touch pad, which shows an ON/OFF voltage ratio of 65 (0.038 V in the OFF state and 2.5 V in the ON state) (Figure 6d). For a stretchable touch pad, we also investigated the ON/OFF voltage ratio using 40% stretched NNH_2 film, since the mechanical durability of the transparent conductors is very important for the operation of flexible touch panels. The ON/OFF voltage ratio of the stretched film is around 24.6 (0.15 V in the OFF state, 3.8 V in the ON state) (Figure 6c). In this regard, it is highly expected that the new stretchable PDMS touch pad can be applied to a real touch screen prototype.

6. Conclusion

The integration of AgNWs onto well-ordered and high density silane modified PDMS substrate has been achieved for mechanically improved transparent conductive films. We successfully demonstrated a permanently silanized surface modification of PDMS with 5 different functional head groups, including NNH_2-, NH_2-, SH-, Cl-, and O-silane derivatives, through a simple, easy, and cheap self-assembly technique. As expected, stronger sigma-donating functional head groups allowed for closer AgNW junction contacts through strong coordination-type bonding between AgNW and the molecularly signalized PDMS, exhibiting a uniform surface of the AgNW network and a prolonged hydrophilicity, and finally producing high conductivity and high stability in a highly stretched state. It is believed that a large amount of aligned functional groups, which can chemically bond with AgNWs, promote permanent adhesion on junction side and lead to excellent electrical and mechanical properties in real device. Thus, this film can be applied to a

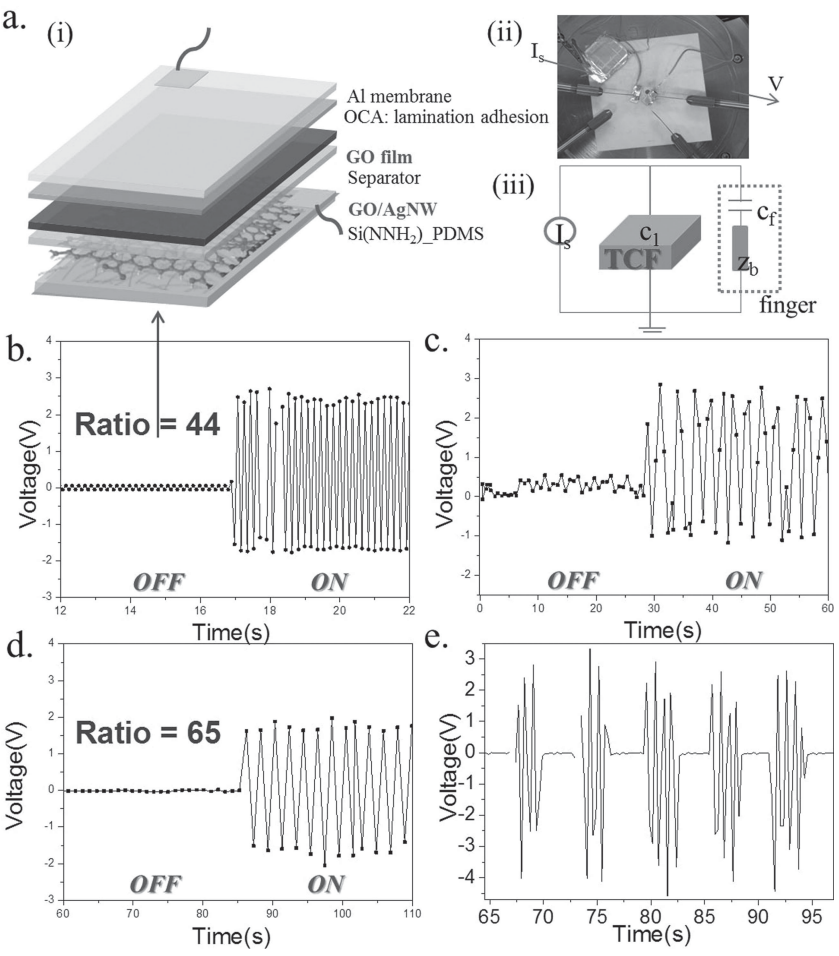

Figure 6. a) Schematic structure of capacitive AgNW PDMS touch pad. GO coated as a separator is laid on a GO/AgNW/Si(NNH_2)/PDMS and then Al membrane is placed (i) and photograph of a real demonstration (ii). Electrical circuit design with the coupling of the finger (iii). (b-e) Measured electrical responses before and after finger touch ($I_s = 10^{-10}$ A). The ON/OFF ratio is ≈44 for AgNW/PDMS (b), ≈24.6 for a 40% stretched AgNW/PDMS (c), and ≈65 for ITO/Glass touch pad (d). e) Sensitivity test for 0.5-Hz touch frequency.

wide variety of the stretchable and wearable solar cells, flexible displays and many other stretchable bio-electrodes.

7. Experimental Section

Materials: Silicone kit(SYLGARD 184), silver nanowires(ClearOhm with average diameter: 30 nm, length: 25 μm) and graphene oxide were used in this study. The GO nanosheets described in a previous report[23] (flake size ≈ 0.05 mm, single layer) were prepared using a modified Hummers method,[24] and nanowires were deposited on films by Samsung Electro-Mechanics (Suwon, Korea). [3-(2-aminoethylamino)propyl] trimethoxysilane (NNH_2), 3-Aminop ropyltriethoxysilane(NH_2), 3-Mercaptopropyltrimethoxy silane (SH), 3-Glycidyloxypropyltrimethoxysilane (O), and 3-Chloropropyltriethoxysila ne(Cl) were purchased from Sigma-Aldrich, and used as received.

Preparation of PDMS Based TCF: PDMS (SYLGARD 184, Dow Coming) was mixed at a 10: 1 weight ratio.[25] PDMS substrate was pretreated with 50-sccm O_2/Argon plasma for 60 s to generate free surface oxygen groups (FEMTO Science, KOREA). Then, this layer was covalently provided with several functional groups by incubation with 10% (NNH2, NH2, SH, O, and Cl) silane solutions in ethanol, and heating to 60 °C for 90 min. Depending on reaction temperature, PDMS showed different mopholgy (Figure S3, Supporting Information). Subsequently, substrates were dipped and washed with ethanol. AgNW and GO were deposited one by one on this silanized PDMS film. 0.5 mg mL^{-1} of AgNW aqueous solution was spin-coated at 500 rpm for 90 s, which was repeated 3×. The resulting AgNW/Silane/PDMS film was then dried in an oven at 65 °C for 30 min. Finally, 0.1 mL of GO nanosheets in aqueous solution (concentration = 0.1 mg mL^{-1}) was spin-coated at 4000 rpm onto the AgNW/Silane/PDMS film.

Characterization of Samples: To measure the resistance and electrical stability of GO/AgNW/Silane/PDMS film, 5-nm Ti/50-nm Au top electrodes with a distance of ≈130 mm were deposited by an E-beam evaporation. The R_{sh} values of these films were measured with a Keithley 4200 semiconductor characterisation system at room temperature under vacuum. The bendabilities of GO/AgNW/Silane/PDMS film were analysed using a custom bending test system. Two terminal measurements were used to monitor the change in resistance of each film. The curvature radius of the bended film was about 1 cm. The R_{sh} values were recorded when the film is straight. The morphologies of each sample were characterised by SEM (FEI NOVA NanoSEM 200 or JEOL JSM-7600F), AFM (Digital Instruments D3100, PSIA XE-100 or Agilent 5500 AFM/SPM), and OM (Olympus BX51, Microscopes Inc. wm003900a S39a, or Sometech Vision Camscope). WCA measurements were performed to determine the wettability of the film surfaces using an SEO Phoenix 300 microscope. The optical transmission and reflectance profiles of the films were recorded on a Varian Cary 5000 UV-Vis spectrophotometer and a Konica Minolta Horizontal Spectrophotometer CM-3600D. Linear raman spectra was measured on a Jobin Yvon/Horiba LabRAM Aramis Raman microscope equipped with a 633-nm laser. AFM – Raman spectra was measured on a NTEGRA Spectra PNL instrument with a 633 nm laser (mapping software: LabSpec5). A VG Microtech ESCA 2000 equipped with a Mg/Al source was used to analyse the surface chemical bonding states M).[26]

Supporting Information

Supporting Information is available from the Wiley Online Library or from the author.

Acknowledgements

This work was supported by the National Research Foundation of Korea (NRF) grant funded by the Korea government (MSIP) (Grant No. 2006–0050684) and partially by the grapheneall company.

Received: September 23, 2013
Revised: December 14, 2013
Published online: February 10, 2014

[1] J. Zang, S. Ryu, N. Pugno, Q. Wang, Q. Tu, M. J. Buehler, X. Zhao, *Nat. Mater.* **2013**, *12*, 321.
[2] S. Park, G. Wang, B. Cho, Y. Kim, S. Song, Y. Ji, M.-H. Yoon, T. Lee, *Nat. Nanotechnol.* **2012**, *7*, 438.
[3] S. H. Chae, W. J. Yu, J. J. Bae, D. L. Duong, D. Perello, H. Y. Jeong, Q. H. Ta, T. H. Ly, Q. A. Vu, M. Yun, X. Duan, Y. H. Lee, *Nat. Mater.* **2013**, *12*, 403.
[4] a) D.-H. Kim, J.-H. Ahn, W. M. Choi, H.-S. Kim, T.-H. Kim, J. Song, Y. Y. Huang, Z. Liu, C. Lu, J. A. Rogers, *Science* **2008**, *320*, 507; b) S. P. Lacour, S. Wagner, H. Zhenyu, Z. Suo, *Appl. Phys. Lett.* **2003**, *82*, 2404.
[5] H. Schmid, B. Michel, *Macromolecules* **2000**, *33*, 3042.
[6] A. Mata, A. Fleischman, S. Roy, *Biomed. Microdevices* **2005**, *7*, 281.
[7] J. C. McDonald, G. M. Whitesides, *Acc. Chem. Res.* **2002**, *35*, 491.
[8] H. T. Ng, M. L. Foo, A. Fang, J. Li, G. Xu, S. Jaenicke, L. Chan, S. F. Y. Li, *Langmuir* **2001**, *18*, 1.
[9] a) A. C. C. Esteves, J. Brokken-Zijp, J. Laven, H. P. Huinink, N. J. W. Reuvers, M. P. Van, G. de With, *Polymer* **2009**, *50*, 3955; b) H. Hillborg, J. F. Ankner, U. W. Gedde, G. D. Smith, H. K. Yasuda, K. Wikström, *Polymer* **2000**, *41*, 6851.
[10] J. Zhou, D. A. Khodakov, A. V. Ellis, N. H. Voelcker, *Electrophoresis* **2012**, *33*, 89.
[11] H. Hakkinen, *Nat. Chem.* **2012**, *4*, 443.
[12] P.-J. Wipff, H. Majd, C. Acharya, L. Buscemi, J.-J. Meister, B. Hinz, *Biomaterials* **2009**, *30*, 1781.
[13] T. Akter, W. S. Kim, *ACS Appl. Mater. Interfaces* **2012**, *4*, 1855.
[14] M. D. Losego, M. E. Grady, N. R. Sottos, D. G. Cahill, P. V. Braun, *Nat. Mater.* **2012**, *11*, 502.
[15] Z. Deng, M. Chen, L. Wu, *J. Phys. Chem. C* **2007**, *111*, 11692.
[16] P. Jiang, S.-Y. Li, S.-S. Xie, Y. Gao, L. Song, *Chem. Eur. J.* **2004**, *10*, 4817.
[17] I. K. Moon, J. I. Kim, H. Lee, K. Hur, W. C. Kim, H. Lee, *Sci. Rep.* **2013**, 3.
[18] H. M. Lee, H. B. Lee, D. S. Jung, J.-Y. Yun, S. H. Ko, S. B. Park, *Langmuir* **2012**, *28*, 13127.
[19] F. Xu, Y. Zhu, *Adv. Mater.* **2012**, *24*, 5117.
[20] A. D. Mazzeo, W. B. Kalb, L. Chan, M. G. Killian, J.-F. Bloch, B. A. Mazzeo, G. M. Whitesides, *Adv. Mater.* **2012**, *24*, 2850.
[21] L. Kogut, K. Komvopoulos, *J. Appl. Phys.* **2004**, *95*, 576.
[22] H. Tian, Y. Yang, D. Xie, T.-L. Ren, Y. Shu, C.-J. Zhou, H. Sun, X. Liu, C.-H. Zhang, *Nanoscale* **2013**, *5*, 890.
[23] I. K. Moon, J. Lee, R. S. Ruoff, H. Lee, *Nat. Commun.* **2010**, *1*, 73.
[24] W. S. Hummers, R. E. Offeman, *J. Am. Chem. Soc.* **1958**, *80*, 1339.
[25] S. H. Tan, N.-T. Nguyen, Y. C. Chua, T. G. Kang, *Biomicrofluidics* **2010**, *4*, 032204.
[26] M. S. Choi, S. H. Lee, W. J. Yoo, *J. Appl. Phys.* **2011**, *110*, 073305.